Inorganic Chemistry

Article

pubs.acs.org/IC

X-ray Absorption Spectroscopy Proves the Trigonal-Planar Sulfur-Only Coordination of Copper(I) with High-Affinity Tripodal Pseudopeptides

Anne-Solène Jullien,[†] Christelle Gateau,[†] Isabelle Kieffer,[‡,§] Denis Testemale,[‡,⊥] and Pascale Delangle*[,†]

[†]Service de Chimie Inorganique et Biologique (UMR_E 3 CEA UJF), Commissariat à l'Energie Atomique et aux Energies Alternatives, INAC, 17 rue des martyrs, 38054 Grenoble Cedex 9, France

[‡]BM30B/FAME beamline, European Synchotron Radiation Facility (ESRF), F-38043 Grenoble Cedex 9, France

[§]Observatoire des Sciences de l'Université de Grenoble, UMS 832 CNRS Université Joseph Fourier, F-38041 Grenoble Cedex 9, France

[⊥]Institut Néel, CNRS et Université Joseph Fourier, BP 166, F-38042 Grenoble Cedex 9, France

Supporting Information

ABSTRACT: A series of tripodal ligands **L** derived from nitrilotriacetic acid (NTA) and extended by three converging metal-binding cysteine chains were previously found to bind selectively copper(I) both in vitro and in vivo. The ligands $\mathbf{L^1}$ (ester) and $\mathbf{L^2}$ (amide) were demonstrated to form copper(I) species with very high affinities, close to that reported for the metal-sequestering metallothioneins (MTs; log $K^{Cu\text{-}MT} \approx 19$). Here, an in-depth study by Cu K-edge X-ray absorption spectroscopy (XAS) was performed to completely characterize the copper(I) coordination sphere in the complexes, previously evidenced by other physicochemical analyses. The X-ray absorption near-edge structure (XANES) spectra shed light on the equilibrium between a mononuclear complex and a cluster for both $\mathbf{L^1}$ (ester) and $\mathbf{L^2}$ (amide). The exclusive symmetric CuS_3 geometry adopted in the mononuclear complexes (Cu−S ≈ 2.23 Å) was clearly demonstrated by extended X-ray absorption fine structure (EXAFS) analyses. The EXAFS analyses also proved that the clusters are organized on a symmetric CuS_3 core (Cu−S ≈ 2.26 Å) and interact with three nearby copper atoms (Cu---Cu ≈ 2.7 Å), consistent with the Cu_6S_9-type clusters previously characterized by pulsed gradient spin echo NMR spectroscopy. XAS data obtained for other architectures based on the NTA template ($\mathbf{L^3}$ acid, $\mathbf{L^4}$ without a functionalized carbonyl group, etc.) demonstrated the formation of polymetallic species only, which evidence the necessity of the proximal ester or amide group to stabilize the CuS_3 mononuclear species. Finally, XAS was demonstrated to be a powerful method to quantify the equilibrium between the two copper(I) environments evidenced with $\mathbf{L^1}$ and $\mathbf{L^2}$ at different copper concentrations and to determine the equilibrium constants between these two complexes.

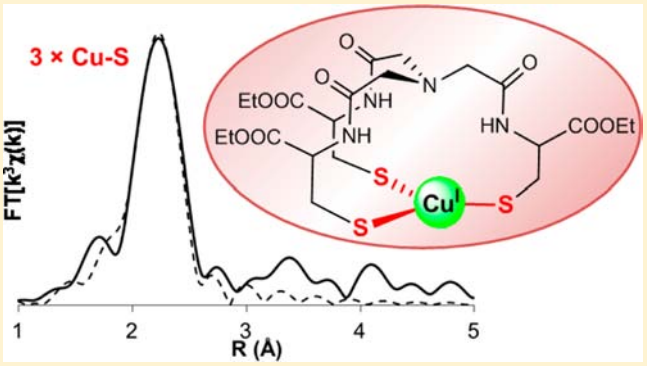

INTRODUCTION

Metal overload is involved in several diseases and intoxications.[1] Among the metals that can accumulate in the body, copper is an essential element used as a cofactor by many redox proteins. However, free copper can also promote Fenton-like reactions and thus can be toxic. That is why the intracellular concentration of copper is rigorously tuned in the body.[2,3] Actually, one of the major genetic disorders of copper metabolism is Wilson's disease, which results in copper overload.[4,5] Chelation therapy has been found to be quite efficient in many cases to treat this disease. Nevertheless, new and more efficient treatments are necessary because many current drugs induce side effects, mainly due to a lack of specificity.[4−7] We have been involved for a few years in the development of intracellular copper(I) chelators that could provide innovative and specific treatments of Wilson's disease.[5] Indeed, because the cytoplasm is a reducing environment, the predominant oxidation state of copper in cells is Cu^I.[8] The copper(I) chelators are inspired from proteins involved in copper homeostasis such as metallochaperones[2,9] and metallothioneins (MTs),[10−13] and therefore the copper(I) binding site is based on cysteines.[14,15] Some of these copper(I) chelators have been targeted to the hepatocytes to localize their activity because the main organ of copper accumulation in Wilson's disease is the liver. Promising results have been obtained because the targeted molecules have been demonstrated to be able to effectively chelate excess intracellular copper.[16,17]

Received: May 14, 2013
Published: August 12, 2013

   dx.doi.org/10.1021/ic401206u | *Inorg. Chem.* 2013, 52, 9954−9961

We recently developed a series of tripodal derivatives based on a nitrilotriacetic acid (NTA) scaffold extended with three converging cysteine groups (Figure 1).[18,19] We established that

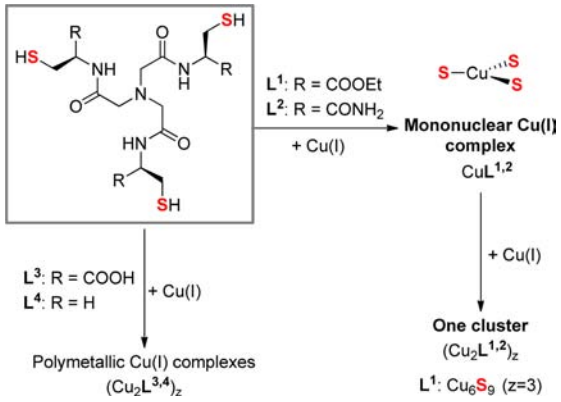

Figure 1. Copper(I) complexes with the tripodal ligands $\mathbf{L^1}$–$\mathbf{L_4}$.

the two ligands $\mathbf{L^1}$ (ester) and $\mathbf{L^2}$ (amide) promote the formation of very stable copper(I) complexes, with a large selectivity with respect to zinc(II), another cation highly present in cells. A variety of spectroscopic methods—UV spectroscopy, circular dichroism (CD), mass spectrometry (MS), and nuclear magnetic resonance (^{1}H/^{13}C NMR)—were used to characterize the copper(I) complexes formed with these two ligands, which demonstrate very similar binding properties: a very stable mononuclear complex, Cu**L**, is formed and transforms into a unique cluster, $(Cu_2\mathbf{L})_3$, in excess of metal ion.[18,19] Moreover, the diffusion coefficients measured by NMR using a pulsed gradient spin echo (PGSE) sequence provided the molecularity of these complexes. It was evidenced that the chelators **L** form $(Cu_2\mathbf{L})_3$ clusters based on Cu_6S_9 cores, as found in the β domains of some MTs,[12,20] which are small cysteine-rich proteins, forming metal clusters and biosynthesized in the presence of toxic metal ions or essential metals such as copper and zinc in excess of physiological requirements. These structural similarities with MTs were found to be related to the high affinities of both $\mathbf{L^1}$ and $\mathbf{L^2}$ for copper(I) in the mononuclear complexes ($\log K^{CuL^1,CuL^2}$ = 19.2 and 18.8)[18,19] close to those reported for MTs in the literature ($\log K^{Cu\text{-}MT} \approx 19$).[21,22]

On the contrary, $\mathbf{L^3}$ (Figure 1), which is functionalized with three carboxylate units, was found to only form polymetallic species. The mononuclear complex with $\mathbf{L^3}$ was not observed, which may be assigned to charge repulsions between the three negatively charged groups at physiological pH in the tripodal ligand.[18]

The soft sulfur ligands $\mathbf{L^1}$–$\mathbf{L^3}$ were also found to be efficient mercury chelating agents, and we demonstrated previously by low-temperature Hg L-edge X-ray absorption spectroscopy (XAS) that the apparent average C_3 symmetry of the HgS_3 environment evidenced by NMR at 298 K was, in fact, a highly distorted geometry with three Hg–S bonds with very different lengths.[23] These data suggested that the NTA-based tripods are too constrained to accommodate a trigonal-planar geometry around the large mercury(II) cation. In fact, the apparent symmetrical species detected by NMR at 298 K mostly results from an average of highly dissymmetric complexes (distorted T shape) that rapidly equilibrate on the NMR time scale at 298 K. That is why we wondered whether such a fast equilibrium could be responsible for the apparent symmetry of the copper(I) complexes observed at the NMR time scale at 298 K. So, to ensure the C_3 symmetry in the copper(I) complexes, Cu K-edge XAS at cryogenic temperature was used.

In this paper, we aim at presenting a complete XAS study of the copper(I) species formed with the tripodal ligands $\mathbf{L^1}$ and $\mathbf{L^2}$, which are promising intracellular copper(I) chelating agents. Ligand $\mathbf{L^3}$ and the new compound $\mathbf{L^4}$, derived from cysteamine (Figure 1), which form only polymetallic species, were also investigated to evaluate the general impact of the NTA template on the copper(I) cluster species formed in solution. For both $\mathbf{L^1}$ and $\mathbf{L^2}$, X-ray absorption near-edge structure (XANES) spectra provide evidence of trithiolato trigonal environments around the copper(I) ion in the mononuclear complexes, whereas extended X-ray absorption fine structure (EXAFS) analyses give direct proof of the symmetric trigonal-planar coordination of copper(I) with three sulfur atoms at average distance Cu–S ≈ 2.23 Å, characteristic of symmetric CuS_3 complexes.[24−26] The polymetallic species are also organized on a CuS_3 core, with typical distances Cu–S ≈ 2.26 Å, which interacts with three nearby copper atoms at an average distance Cu---Cu ≈ 2.7 Å, as in many copper(I) transport proteins such as Atox1,[26,27] Cox17,[28,29] Mac1, Ace1,[30] Amt1,[31] Ctr1,[32] MTs,[33−35] and many inorganic model clusters.[36] Moreover, analyses of edge spectra allowed us to quantify the amount of mononuclear and polymetallic species formed in solution with both $\mathbf{L^1}$ and $\mathbf{L^2}$ and confirmed the partial formation constants K_{63} of the polynuclear species $(Cu_2\mathbf{L^{1-2}})_3$ ($\log K_{63}^{L^1}$ = 20.8 and $\log K_{63}^{L^2}$ = 21.5). These results are in very good agreement with data previously obtained by competition experiments with bathocuproine disulfonate (BCS).[18,19] Therefore, both EXAFS and XANES analyses provided very powerful tools to fully characterize the copper(I) complexes formed with the tripodal pseudopeptides in terms of both structures and affinities.

EXPERIMENTAL SECTION

Sample Preparation. The syntheses of the ligands $\mathbf{L^1}$ (ester), $\mathbf{L^2}$ (amide), and $\mathbf{L^3}$ (acid) were described elsewhere.[18,19] The synthesis of $\mathbf{L^4}$ (without functionalized carbonyl group R; Figure 1) is reported in the Supporting Information (SI). The whole set of samples **L** was prepared in a phosphate buffer (100 mM, pH 7.4)/glycerol/acetonitrile (70:20:10, v/v/v) mixture, and the final concentration of the ligand **L** solution was determined by measuring the free thiol concentration following Ellman's procedure.[37] This procedure uses 5,5′-dithiobis(2-nitrobenzoic acid) (DTNB) as an indicator. Each free thiol group present in the peptide yields 1 equiv of TNB^{2-} [λ = 412 nm, $\varepsilon(TNB^{2-})$ = 14150 M^{-1} cm^{-1}]. The copper(I) solutions were prepared by dissolving the appropriate amount of $Cu(CH_3CN)_4{\cdot}PF_6$ in deoxygenated acetonitrile. The final concentration was determined by adding an excess of sodium bathocuproine disulfonate (Na_2BCS) and measuring the absorbance of $Cu(BCS)_2^{3-}$ (λ_{max} = 483 nm, ε = 13300 M^{-1} cm^{-1}).[32] Then, aliquots corresponding to x equiv of copper(I) (0.5 < [Cu^I] < 5 mM, i.e., 0.15–2 equiv) were added to the ligand solution. Because the samples were sensitive to oxygen, the preparations were performed in a glovebox before each XAS experiment. Then, the samples were transferred to the XAS beamline under an argon atmosphere to avoid any oxidation. Drops (50 μL) of the solutions were then deposed on the sample holders, frozen in liquid nitrogen, and placed in a helium cryostat to be analyzed by XAS at Cu K-edge (8979 eV). The compositions of the samples are reported in Table 1.

XAS. XAS measurements were carried out at the European Synchrotron Radiation Facility (ESRF, Grenoble, France), which was operating with a ring current of 200 mA. Cu K-edge XAS spectra

dx.doi.org/10.1021/ic401206u | Inorg. Chem. 2013, 52, 9954−9961

Table 1. List of Samples Analyzed by XAS in a Phosphate Buffer (100 mM, pH 7.4)/Glycerol/Acetonitrile (70:20:10, v/v/v) Mixture

ligand	sample	[L] (mM)	[Cu^I] (mM)	Cu/L
L^1	1A	2.75	0.50	0.18
	1B	2.68	1.25	0.47
	1C	2.61	2.00	0.77
	1D	2.46	3.50	1.41
	1E	2.39	4.25	1.78
	1F	2.43	4.83	1.98
L^2	2A	3.08	0.50	0.16
	2B	2.90	0.74	0.25
	2C	2.81	1.41	0.50
	2D	2.97	1.50	0.51
	2E	2.81	2.50	0.89
	2F	2.75	3.50	1.27
	2G	2.65	4.50	1.70
	2H	2.47	5.00	2.00
L^3	3A	2.76	2.50	0.92
L^4	4A	2.25	1.12	0.50
	4B	2.04	3.05	1.50

were collected at the BM30B (FAME) beamline using a Si(220) double-crystal monochromator with dynamic sagittal focusing. The photon flux was on the order of 10^{12} photons s^{-1}, and the spot size was full-width at half-height (fwhm) 300 μm horizontal × 150 μm vertical.[38] The sample holder was loaded in a helium cryostat with the temperature set to 10 K in order to avoid X-ray beam damage of the sample during data collection. The spectra were collected in fluorescence mode by measuring the Cu Kα fluorescence with a 30-element solid-state germanium detector (Canberra). From 4 to 10 scans, depending on the copper concentration in the sample, 40 min each were averaged. Data from each detector channel were inspected for glitches or dropouts before inclusion in the final average. The energy calibration was achieved by measuring a metallic copper foil for the Cu edge and assigning the first inflection point of the copper foil spectrum to 8979 eV.

The data analyses were performed using the *Horae* package,[39] including *ATHENA* for the data extraction and *ARTEMIS* for the shell fitting. XANES spectra were background-corrected by a linear regression through the preedge region and a low-order polynomial curve through the postedge region and normalized to the edge jump. The spectra for **L**-based copper(I) species were compared qualitatively to the reference spectra for copper(I)-based thiolate complexes available in the literature.[26−36] For extraction of the EXAFS, the threshold energy E_0 was defined at the half-height of the absorption edge step. A cubic spline was fitted through the EXAFS energy range and subtracted to remove the background. The k^3-weighted EXAFS spectra were Fourier-transformed over the k range 2−13 $Å^{-1}$ using a Hanning window. The upper limit of the k range, 13 $Å^{-1}$, was chosen to avoid signals from minute traces of zinc (threshold 9660 eV, i.e., 13 $Å^{-1}$) always present in liquid samples.[36] The fits were performed on the Fourier-transformed spectra over the R range 1−3 Å. Two structural fit models were then applied. The first one (a coordinate-based model) was derived from the atomic coordinates of the sulfur and copper atoms in the $[Cu_4\ (CH_3S^-)_6]^{2-}[(C_3H_7)_4N^+]_2$ cluster described by Baumgartner et al. (see Table S1, SI).[40] On the basis of this structure, for the mononuclear complexes, the atomic coordinates of Cu(1), S(1), S(2), and S(3) were used in *Atoms* (*ARTEMIS* module). For the clusters, data were fitted using a model based on the whole set of copper and sulfur coordinates because in this case one copper atom is surrounded by three sulfur and three copper atoms, as expected for the **L**-based copper(I) clusters. The second model consisted of using structural tetrahedral models (see the SI for further information). In each case, the coordination number was set to 3 for sulfur atoms in the mononuclear complexes and 3 for both sulfur and copper atoms in the clusters. The amplitude reduction factor S_0^2 was set to 0.9 because this value was reported for CuS_3 model compounds also studied at the BM30B (Fame) and here chosen as references.[26] Then the distances Cu−S and Cu−Cu (Å), the Debye−Waller factor (σ^2 in $Å^2$), and the goodness-of-fit (χ_n^2) values were compared to data reported for model compounds to assert the validities of the EXAFS fitting results.[26−36]

RESULTS

Most of the results are presented for the ester ligand L^1. Similar data were obtained with the amide ligand L^2 and are therefore mainly presented in the SI.

Copper K-Edge Spectral Analyses. Several copper complexes have been extensively studied by XAS, and a large amount of data are available in the literature.[26−36,41] In particular, it is well-known that a peak centered at 8982−8985 eV in the XANES region accounts for the existence of copper(I) species. This peak can be interpreted in terms of ligand-field theory. The transitions from the 1s orbital to the 4p orbitals of the copper(I) ion are responsible for the absorption observed in the 8982−8985 eV area of the spectrum (Figure 2).[42] Both the peak intensity and the peak energy position

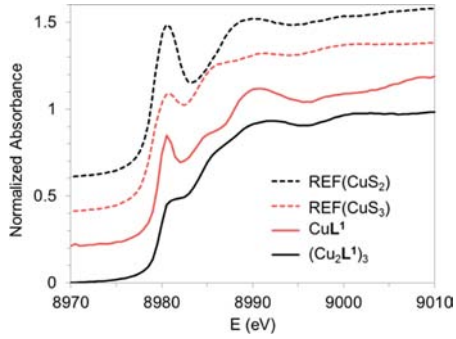

Figure 2. Normalized Cu edge spectra of copper(I) references (linear REF(CuS_2) = $[Et_4N][Cu(SAd)_2]$ and trigonal REF(CuS_3) = $[Et_4N]_2[Cu(SC_6H_4\text{-}p\text{-}Cl)_3]$) and experimental spectra of L^1-based copper(I) species [CuL^1 = sample 1A and $(Cu_2L^1)_3$ = sample 1F]. Spectra are offset for clarity.

depend on the ligands that bind the copper(I) ion. Actually, both the atom types and the coordination sphere around the copper(I) ion determine the shape of the peak as seen on the spectra of copper(I) reference compounds given in Figure 2. In the complex $[Et_4N][Cu(SAd)_2]$,[26,41,43] the copper(I) ion is linearly coordinated to two sulfur atoms, and the peak appears sharp and intense [REF(CuS_2) in Figure 2].[26] By contrast, the peak intensity related to the complex $[Et_4N]_2[Cu(SC_6H_4\text{-}p\text{-}Cl)_3]$,[25,26] where copper(I) is trigonally coordinated by three sulfur atoms, is weaker [REF(CuS_3) in Figure 2].

The spectra of these reference compounds in the solid state[26] are compared with those of copper(I) complexes of L^1 in solution in Figure 2. Clearly, the spectrum obtained for the mononuclear complex CuL^1, which is the species present in excess of ligand, i.e., in sample 1A (Table 1), shows strong similarities with the spectrum recorded for the trigonally coordinated copper(I) in $[Et_4N]_2[Cu(SC_6H_4\text{-}p\text{-}Cl)_3]$ [REF(CuS_3) in Figure 2]. These two spectra display very similar intensities (~0.65−0.68) of the peak centered at 8982−8985 eV and similar relative intensities and positions of the XANES peaks in general. This suggests that the central copper(I) ion is trigonally bound to the three sulfur atoms of the ligand scaffold in the mononuclear complex CuL^1. In excess of copper(I), the spectrum is different and the peak intensity collapses

dx.doi.org/10.1021/ic401206u | Inorg. Chem. 2013, 52, 9954−9961

completely when 2 equiv of copper(I) is added to $\mathbf{L}^1$ in sample 1F (Table 1 and Figure 2). This is consistent with formation of the cluster $(Cu_2\mathbf{L}^1)_3$, in which the environment of the central copper(I) ion differs from the one found in the mononuclear complexes. For intermediate concentrations of copper(I), the intensity of the peak centered at 8982 eV decreases gradually before the final collapse for 2 equiv of copper(I) added. This phenomenon is depicted in Figure 3 for $\mathbf{L}^1$.

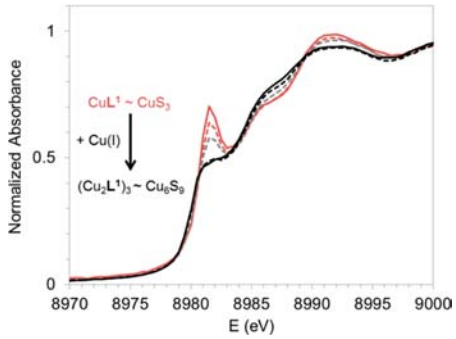

Figure 3. Normalized Cu edge spectra obtained for ligand $\mathbf{L}^1$ with increasing amounts of copper(I).

The analogous graph for $\mathbf{L}^2$ is reported in Figure S1 in the SI. This regular decrease clearly indicates that the cluster is forming at the expense of the mononuclear complex when the copper concentration increases in solution. Besides, isosbestic points in the edge area of the spectra (Figure 3) are detected at 8981, 8984, and 8988 eV, which demonstrates the presence of only two copper(I) complexes in equilibrium. These observations corroborate previous physicochemical studies (UV, CD, MS, $^1H/^{13}C$ NMR, and PGSE-NMR), which have shown that both $\mathbf{L}^1$ and $\mathbf{L}^2$ form mononuclear complexes and the clusters $(Cu_2\mathbf{L}^1)_3$ and $(Cu_2\mathbf{L}^2)_3$ in solution.[18,19]

By contrast, $\mathbf{L}^3$ (Figure 1) was shown to be unable to form mononuclear complexes in solution, even at low concentrations of copper and would rather complex copper in $(Cu_2\mathbf{L}^3)_z$ polymetallic species.[18] Similar observations were obtained with the analogue $\mathbf{L}^4$. As expected, the peak centered at 8982 eV in the XAS spectra of these complexes was very flat and the shapes of the curves were similar to the one observed for the clusters $(Cu_2\mathbf{L}^1)_3$ and $(Cu_2\mathbf{L}^2)_3$ in samples 1F and 2H (Figure 4), even in excess or stoichiometric amounts of the ligand. Unfortunately, it was not possible to determine the

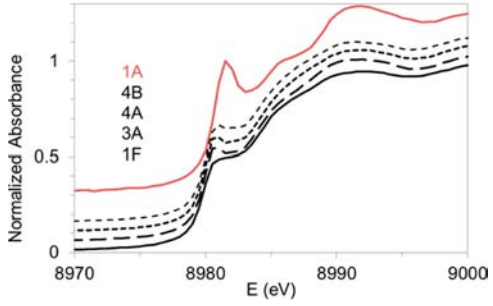

Figure 4. Normalized Cu edge spectra of $\mathbf{L}^1$ complexes—Cu$\mathbf{L}^1$ (sample 1A) and $(Cu_2\mathbf{L}^1)_3$ (sample 1F)—compared to the spectra measured for Cu$\mathbf{L}^3$ (sample 3A; 1 equiv of copper) and Cu$\mathbf{L}^4$ (samples 4A and 4B; 0.5 and 1.5 equiv of copper, respectively) species. Spectra are offset for clarity.

molecularities (z) of the clusters $(Cu_2\mathbf{L}^3)_z$ and $(Cu_2\mathbf{L}^4)_z$ by diffusion coefficient measurements by NMR because the ^1H NMR signals of the complexes with $\mathbf{L}^3$ or $\mathbf{L}^4$ were too large. Anyway, the lack of an amide or ester function next to the coordinating thiolate functions of $\mathbf{L}$ (Figure 1) is responsible for the absence of well-defined mononuclear complexes in solution with both $\mathbf{L}^3$ and $\mathbf{L}^4$.

To characterize the copper(I) species formed in solution and refine the coordination spheres around the copper(I) ion in each case, the EXAFS domains of the XAS spectra were then looked into. The EXAFS data of the mononuclear complexes Cu$\mathbf{L}^1$ and Cu$\mathbf{L}^2$ were analyzed in samples 1A and 2A with low copper(I) concentrations. The clusters $(Cu_2\mathbf{L}^1)_3$ and $(Cu_2\mathbf{L}^2)_3$ were investigated in samples 1F and 2H, which contain 2 equiv of copper(I). Both samples 1A (or 2A) and 1F (or 2H) were shown previously by ^1H NMR to contain only the mononuclear adduct and the polymetallic one, respectively.

EXAFS Analyses: Mononuclear Complexes of $\mathbf{L}^1$ and $\mathbf{L}^2$. The EXAFS fitting results obtained for the mononuclear complex Cu$\mathbf{L}^1$ are depicted in Figure 5a. Similar graphs were obtained for the mononuclear complex Cu$\mathbf{L}^2$ (Figure S2, SI). Clearly, the model based on a central copper atom surrounded by three sulfur atoms in a trigonal-planar geometry[40] returns a very good fit of the data collected. The quantitative results are reported in Table 2. Importantly, models with only two sulfur atoms in a digonal geometry give significantly poorer results, and models with a T-shaped coordination return nonphysical negative Debye−Waller values. The three S−Cu distances were found to be almost equal, at ≈2.23 Å (Table 2). This distance belongs to the characteristic distance range reported for symmetric CuS_3 compounds, ≈2.22−2.26 Å, in the literature.[24−26] Consequently, these data confirm that both $\mathbf{L}^1$ and $\mathbf{L}^2$ form mononuclear complexes with a typical symmetric CuS_3 coordination. This demonstrates that the NMR spectra recorded at 298 K[17,18] are characteristic of C_3-symmetric mononuclear copper(I) complexes and are not the result of dissymmetric species averaged at the NMR time scale at 298 K like with mercury(II).[23]

EXAFS Analyses: Polymetallic Species $(Cu_2L)_z$. The EXAFS fitting results obtained for the cluster $(Cu_2\mathbf{L}^1)_3$ are depicted in Figure 5b. Analogous graphs were obtained for the cluster $(Cu_2\mathbf{L}^2)_3$ (Figure S2, SI). The models based on a central copper atom surrounded by three sulfur atoms in a trigonal-planar geometry and three copper atoms[40] give a good fit of the data collected, either using the coordinate-based model or the tetrahedral-based model. In particular, they reproduce the beat at 8 $Å^{-1}$, characteristic of the additional Cu---Cu interactions. The quantitative results are reported in Table 2. The distances Cu−S ≈ 2.26 Å and Cu---Cu ≈ 2.7 Å were found to be in accordance with values given in the literature for several copper(I) proteins,[26−32] in particular MTs,[33−35] and some inorganic model clusters[36] organized on a CuS_3 core, which interact with one to three nearby copper atoms in either Cu_4S_6 or Cu_6S_9 clusters. The Cu---Cu distances obtained with the coordinate-based model are not equal (≈2.65−2.82 Å; see Table 2), but the resolution expected for these second-shell atoms is too low (~0.1 Å)[44] to allow a discrimination between so close distances. Therefore, the tetrahedral-based model, which sets the three copper atoms at the same distance (2.73 Å) from the central copper atom, is preferred.

The EXAFS analyses performed for the copper(I) complexes formed with the ligands $\mathbf{L}^3$ and $\mathbf{L}^4$ gave very similar results (Table 2). The corresponding graphs are depicted in Figure S3

dx.doi.org/10.1021/ic401206u | Inorg. Chem. 2013, 52, 9954−9961

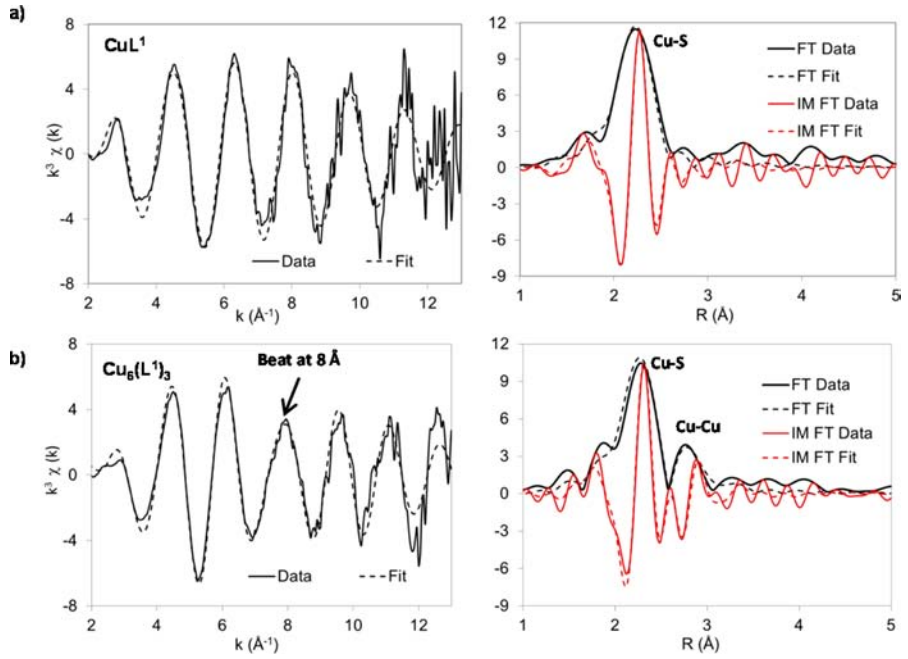

Figure 5. XAS data for (a) the mononuclear complex CuL^1 (sample 1A) and (b) the cluster $(Cu_2L^1)_3$ (sample 1F). Left: Spectra of the k^3-weighted EXAFS experimental data and corresponding fit. Right: Fourier transforms of the k^3-weighted EXAFS experimental data and corresponding fit. FT and IM FT are the real and imaginary parts for Fourier transformation, respectively. Solid lines: experimental data. Dotted lines: fit.

Table 2. EXAFS Fitting Results[a]

complex	sample	3 × Cu−S	$\sigma(S)^2$	3 × Cu−Cu	$\sigma(Cu)^2$	ΔE	χ_n^2	R
CuL^1	1A	2.23	5(1)			4(2)	15	4.0
CuL^2	2A	2.23	5(1)			3(2)	33	7.1
$(Cu_2L^1)_3$	1F[b]	2.26	5(1)	2.65, 2.71, 2.80	10(3)	5(2)	92	4.5
	1F[c]	2.26	5(1)	2.73	15(3)	5(2)	118	7.0
$(Cu_2L^2)_z$	2H[b]	2.26	5(1)	2.66, 2.72, 2.82	9(2)	4(1)	37	2.0
	2H[c]	2.26	5(1)	2.74	14(4)	4(2)	51	2.4
$(Cu_2L^3)_z$	3A[b]	2.26	5(1)	2.66, 2.71, 2.81	5(1)	5(1)	23	2.0
	3A[c]	2.26	4(1)	2.73	10(1)	5(1)	34	2.5
$(Cu_2L^4)_z$	4A[b]	2.26	4(1)	2.66, 2.73, 2.82	5(1)	5(1)	9	1.3
	4A[c]	2.26	4(1)	2.73	10(1)	5(1)	16	2.0

[a]Distances are in angstroms with 0.01 or 0.02 errors for the Cu−S and Cu−Cu distances, respectively. Other experimental errors on the last character are indicated in parentheses. Debye−Waller factors (σ^2) are in $Å^2 \times 10^3$. The threshold energy shifts ΔE are in electronvolts. χ_n^2 and R (%) are the reduced χ^2 and the R factor of the fit, respectively. Samples 1A and 2A (mononuclear complexes) were analyzed with atomic coordinates of Cu(1), S(1), S(2), and S(3) only. [b]Samples 1F, 2H, 3A, and 4A (polynuclear complexes) were analyzed with the whole set of copper and sulfur atomic coordinates of sulfur and copper atoms in the $[Cu_4(CH_3S^-)_6]^{2-}[(C_3H_7)_4N^+]_2$ cluster described by Baumgartner et al.[40] [c]Samples 1F, 2H, 3A, and 4A (polynuclear complexes) were analyzed with the tetrahedral-based model of coordinates (see the Experimental Section).

in the SI. Like the analogous architectures L^1 and L^2, both L^3 and L^4 form polymetallic species based on a symmetric CuS_3 core (Cu−S ≈ 2.26 Å), which interacts with three copper atoms at the distance Cu---Cu ≈ 2.7 Å. These results provide the evidence that, as a main rule, ligands based on the NTA template tend to form the same type of first-shell clusters in solution.

Speciation of the Copper(I) Complexes with L^1 and L^2 from the XANES Spectra. The thermodynamic equilibria for the formation of copper(I) complexes with L^1 and L^2 were shown to be the following:[19]

$$Cu^I + L = CuL \quad (\beta_{11}) \tag{1}$$

$$CuL + Cu^I = \frac{1}{3}(Cu_2L)_3 \quad (K_{63}) \tag{2}$$

The two binding constants were evaluated in previous studies with competition experiments starting from the mononuclear complex or the cluster and adding BCS as a competitor for copper(I).[18,19] The two ligands L^1 and L^2 were found to tightly bind the copper(I) ion in the mononuclear complexes with affinities log β_{11} = 19.2 and 18.8, respectively, close to those determined for MTs (log $K^{Cu\text{-}MT} \approx 19$).[21,22] The equilibrium constant between the mononuclear complexes and the polymetallic ones, K_{63}, was also determined: log K_{63} = 20.7[19] and 21.5[45] for L^1 and L^2, respectively. The expected speciation in the conditions used for the XAS experiments could thus be calculated from these constants with the program *Hyss 2009*[46] and is represented by the dotted red lines in Figure 6.

On the other hand, because the XANES spectra are sensitive to both the nuclearity and geometry of the copper(I) species formed in solution,[36,42] it was possible to calculate the proportions of each complex in the samples. Linear

dx.doi.org/10.1021/ic401206u | Inorg. Chem. 2013, 52, 9954−9961

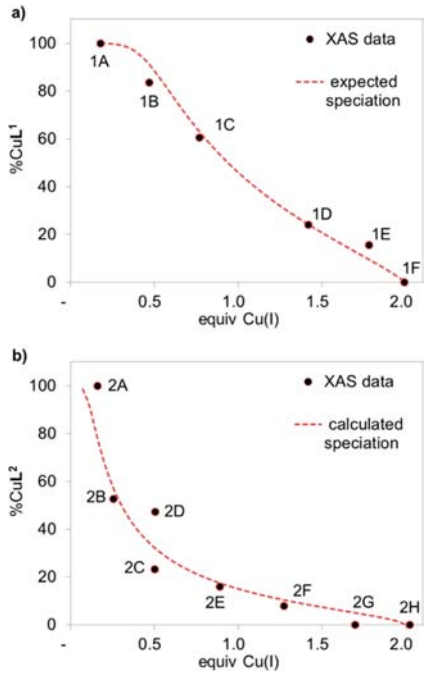

Figure 6. Comparison between the proportions of mononuclear complexes (a) Cu$\mathbf{L}^1$ and (b) Cu$\mathbf{L}^2$, obtained after linear combinations of the XANES spectra in *ATHENA* (black circles) and the proportions calculated from thermodynamic constants obtained from BCS competitions (dotted red lines). (a) $\mathbf{L}^1$: log β_{11} = 19.2, log K_{63} = 20.7, [**L**] = 2.5 mM. (b) $\mathbf{L}^2$: log β_{11} = 18.8, log K_{63} = 21.5, [**L**] = 2.75 mM.

combinations of the extreme XANES spectra obtained for the lowest copper concentration (Table 1, samples 1A or 2A, [Cu]/[**L**] = 0.16−0.18) and the highest copper concentration (Table 1, samples 1F or 2H, [Cu]/[**L**] = 2) were performed with the linear combination module available in *ATHENA*.[47] Indeed, samples 1A (or 2A) and 1F (or 2H) were shown by ^{1}H NMR to contain only the mononuclear adduct and the polymetallic one, respectively. The EXAFS threshold energy E_0 was set at 8980 eV for the whole set of curves. The energy range around the threshold energy was typically restrained to ±10 eV around E_0. An analysis close to E_0 was preferred because the long-range disorder and noise peculiar to each EXAFS spectrum do not affect the edge area. The results are reported in Tables S4 and S5 in the SI for $\mathbf{L}^1$ and $\mathbf{L}^2$, respectively. Figure 6 shows the superimposition of the experimental points derived from the edge analysis and the speciation calculated with the constant values previously obtained from competitions with BCS. The agreement is very satisfying for the two ligands. The constants K_{63} were calculated from the edge data and for samples containing a reasonable amount of the two complexes: log $K_{63}^{\mathbf{L}^1}$ = 20.8 ± 0.1 (for $\mathbf{L}^1$, samples 1B, 1C, and 1D; Table S4, SI) and log $K_{63}^{\mathbf{L}^2}$ = 21.5 ± 0.4 (for $\mathbf{L}^2$, samples 2B−2F; Table S5, SI).

DISCUSSION

The tripodal ligands $\mathbf{L}^1$−$\mathbf{L}^4$ derived from NTA and extended by three converging metal-binding cysteine chains revealed to be very efficient copper(I) chelating agents both in vitro[18,19] and in vivo.[16] Besides, previous physicochemical analyses have shown that two types of copper(I) complexes are formed in a water solution at physiological pH.[17,18] $\mathbf{L}^1$ (ester) and $\mathbf{L}^2$ (amide) exhibit the most interesting copper(I) chelating properties with very high affinities and an equilibrium between a mononuclear complex and a unique polymetallic species $(Cu_2\mathbf{L}^{1-2})_3$.

Cu K-edge XAS was used here to gain insights into the structures of the copper(I) complexes and to completely characterize the coordination sphere of the copper(I) ion. Analyses of the XANES spectra of $\mathbf{L}^1$ and $\mathbf{L}^2$ confirm both the existence of the mononuclear complex at low copper concentration and the equilibrium between only two different copper environments, the mononuclear complex and a unique polymetallic species, as evidenced by several isosbestic points. The exclusive CuS_3 geometry adopted in the mononuclear complexes was clearly supported by EXAFS fitting, which provide three equal distances Cu−S ≈ 2.23 Å, characteristic of symmetric CuS_3 coordination. It is quite interesting to notice that these symmetric copper(I) mononuclear complexes dramatically differ from the dissymmetric analogous mercury(II) mononuclear complexes recently investigated by Hg L-edge XAS spectroscopy.[23] Whereas other spectroscopic methods used at ambient temperature (^{1}H and ^{199}Hg NMR and UV spectroscopy) indicated a trigonal-planar trithiolato coordination of mercury(II), the EXAFS data revealed a dissymmetrical HgS_3 binding environment with three sulfur atoms at 2.38, 2.51, and 2.67 Å (Figure 7, left). Even though

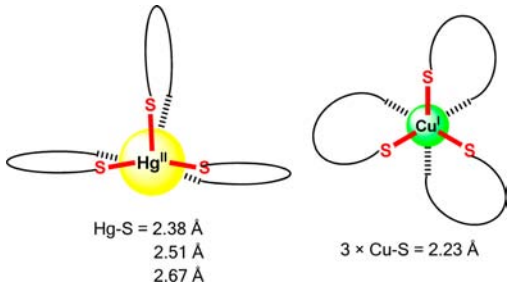

Figure 7. Structures of the coordination spheres of mercury(II) and copper(I) in their mononuclear complexes with $\mathbf{L}^1$ and $\mathbf{L}^2$.

coordination changes upon freezing cannot be totally excluded, this result suggests that the tripodal ligands $\mathbf{L}^1$ and $\mathbf{L}^2$ are too constrained to accommodate a trigonal-planar coordination mode for the large cation mercury(II). On the contrary, the EXAFS data obtained with copper(I) in this work demonstrate that this metal ion is bound by three sulfur atoms in a very symmetric environment, with three identical Cu−S bonds with an average distance Cu−S = 2.23 Å (Figure 7, right). The difference in the metal coordination spheres between mercury(II) and copper(I) complexes may be assigned to their ionic radii: the mercury(II) ionic radius is approximately 50% greater than that of copper(I).[48]

As for the polymetallic species, the EXAFS fitting implemented with the coordinates of a Cu_4S_6 model cluster was found to return good fits of the cluster data, thus demonstrating that the central copper of the clusters is surrounded by three sulfur atoms at equal distances (Cu−S ≈ 2.26 Å) and three copper atoms (Cu---Cu ≈ 2.7 Å). Of course, the EXAFS data do not allow us to distinguish between $(Cu_2\mathbf{L})_z$ clusters of different molecularities (z > 1) because the copper environments are very similar in clusters of different sizes. However, the results are consistent with the structure of the clusters $(Cu_2\mathbf{L}^{1,2})_3$, which were evidenced by diffusion NMR spectroscopy.[18,19] More generally, because the two

dx.doi.org/10.1021/ic401206u | Inorg. Chem. 2013, 52, 9954−9961

ligands $\mathbf{L}^3$ (acid) and $\mathbf{L}^4$ (no substituent R) were also found to form clusters with similar geometries, it was concluded that, as a main rule, the NTA-based chelator **L** tends to form $(Cu_2\mathbf{L}^1)_x$–$(Cu_2\mathbf{L}^4)_z$ clusters as found in copper(I) proteins,[26−32] in particular MTs,[33−35] and some inorganic model clusters.[36] This result provides insight into an efficient design of copper(I) chelators that mimic the coordination sphere found in proteins in either Cu_4S_6 or Cu_6S_9 clusters.[26−36]

In addition to these structural results, the percentage of each species at each step of the titration could be determined by the quantitative linear combination fitting of the XANES spectra. These analyses return the equilibrium constants between the two complexes log K_{63} = 20.8(1) and 21.5(4) for $\mathbf{L}^1$ and $\mathbf{L}^2$, respectively. These values are in total agreement with an independent determination described elsewhere using BCS as a copper(I) competitor.[18,19] Therefore, XANES provides reliable equilibrium constants even at very low copper concentrations (down to 0.5 mM for samples 1A and 2A; Table 1). Moreover, they confirm that the domain of predominance of the mononuclear CuS_3 species is significantly larger for the ester ligand $\mathbf{L}^1$ and that the amide ligand $\mathbf{L}^2$ has a greater tendency to form the cluster from the mononuclear complex, as shown in the speciation diagrams of parts a ($\mathbf{L}^1$) and b ($\mathbf{L}^2$) in Figure 6.

In conclusion, the tripodal ligands **L** derived from NTA and extended by three converging metal-binding cysteine chains are promising copper(I) chelating agents for in vivo applications such as the treatment of Wilson's disease. Here, Cu K-edge XAS gives very important structural information for the two types of copper(I) complexes formed with these ligands. Copper(I) is coordinated by three sulfur atoms in a trigonal-planar environment whatever the nuclearity of the complex is. The C_3-symmetric structure found for the mononuclear complexes suggests that the cavity of the NTA-based tripodes is perfectly adapted to the coordination of copper(I), which is not the case for larger cations such as mercury(II). Thus, the large affinity of these chemical architectures for copper(I) may be attributed to their ability to induce the very stable sulfur-only trigonal-planar copper(I) coordination. Moreover, the copper environment in the cluster $(Cu_2\mathbf{L}^{1,2})_3$ is reminiscent of the geometry found in copper(I) proteins or MTs with Cu---Cu interactions at an average distance of 2.7 Å. These structural data are essential for the design of copper(I) chelators as potential intracellular drugs used to treat copper overloads.

■ ASSOCIATED CONTENT

Ⓢ Supporting Information

Syntheses of ligand $\mathbf{L}^4$ and supplementary figures and tables for the XAS analyses. This material is available free of charge via the Internet at http://pubs.acs.org.

■ AUTHOR INFORMATION

Corresponding Author

*E-mail: pascale.delangle@cea.fr.

Notes

The authors declare no competing financial interest.

■ ACKNOWLEDGMENTS

This research was supported by the "Agence Nationale pour la Recherche" (COPDETOX; Grant ANR-11-EMMA-025), the "Fondation pour la Recherche Médicale" (Grant DCM20111223043), and the Labex ARCANE (Grant ANR-11-LABX-0003-01). The authors acknowledge the ESRF and FAME CRG beamline for provision of the synchrotron radiation beamline and facilities.

■ REFERENCES

(1) Scott, L. E.; Orvig, C. *Chem. Rev.* **2009**, *109*, 4885.
(2) Kim, B. E.; Nevitt, T.; Thiele, D. J. *Nat. Chem. Biol.* **2008**, *4*, 176.
(3) Lutsenko, S. *Curr. Opin. Chem. Biol.* **2010**, *14*, 211.
(4) Huster, D. *Best Pract. Res., Clin. Gastroenterol.* **2010**, *24*, 531.
(5) Delangle, P.; Mintz, E. *Dalton Trans.* **2012**, *41*, 6359.
(6) Andersen, O. *Chem. Rev.* **1999**, *99*, 2683.
(7) Sarkar, B. *Chem. Rev.* **1999**, *99*, 2535.
(8) Tao, T. Y.; Gitlin, J. A. *Hepatology* **2003**, *37*, 1241.
(9) Rosenzweig, A. C.; O'Halloran, T. V. *Curr. Opin. Chem. Biol.* **2000**, *4*, 140.
(10) Koch, K. A.; Pena, M. M. O.; Thiele, D. J. *Chem. Biol.* **1997**, *4*, 549.
(11) Stillman, M. J. *Coord. Chem. Rev.* **1995**, *144*, 461.
(12) Nielson, K. B.; Atkin, C. L.; Winge, D. R. *J. Biol. Chem.* **1985**, *260*, 5342.
(13) Calderone, V.; Dolderer, B.; Hartmann, H. J.; Echner, H.; Luchinat, C.; Del Bianco, C.; Mangani, S.; Weser, U. *Proc. Natl. Acad. Sci. U.S.A.* **2005**, *102*, 51.
(14) Rousselot-Pailley, P.; Seneque, O.; Lebrun, C.; Crouzy, S.; Boturyn, D.; Dumy, P.; Ferrand, M.; Delangle, P. *Inorg. Chem.* **2006**, *45*, 5510.
(15) Seneque, O.; Crouzy, S.; Boturyn, D.; Dumy, P.; Ferrand, M.; Delangle, P. *Chem. Commun.* **2004**, 770.
(16) Pujol, A. M.; Cuillel, M.; Jullien, A.-S.; Lebrun, C.; Cassio, D.; Mintz, E.; Gateau, C.; Delangle, P. *Angew. Chem., Int. Ed.* **2012**, *51*, 7445.
(17) Pujol, A. M.; Cuillel, M.; Renaudet, O.; Lebrun, C.; Charbonnier, P.; Cassio, D.; Gateau, C.; Dumy, P.; Mintz, E.; Delangle, P. *J. Am. Chem. Soc.* **2011**, *133*, 286.
(18) Pujol, A. M.; Gateau, C.; Lebrun, C.; Delangle, P. *Chem.—Eur. J.* **2011**, *17*, 4418.
(19) Pujol, A. M.; Gateau, C.; Lebrun, C.; Delangle, P. *J. Am. Chem. Soc.* **2009**, *131*, 6928.
(20) Presta, A.; Green, A. R.; Zelazowski, A.; Stillman, M. J. *Eur. J. Biochem.* **1995**, *227*, 226.
(21) Faller, P. *FEBS J.* **2010**, *277*, 2921.
(22) Hamer, D. H. *Annu. Rev. Biochem.* **1986**, *55*, 913.
(23) Pujol, A. M.; Lebrun, C.; Gateau, C.; Manceau, A.; Delangle, P. *Eur. J. Inorg. Chem.* **2012**, 3835.
(24) Garner, C. D.; Nicholson, J. R.; Clegg, W. *Inorg. Chem.* **1984**, *23*, 2148.
(25) Fujisawa, K.; Imai, S.; Suzuki, S.; Moro-oka, Y.; Miyashita, Y.; Yamada, Y.; Okamoto, K. *J. Inorg. Biochem.* **2000**, *82*, 229.
(26) Poger, D.; Fillaux, C.; Miras, R.; Crouzy, S.; Delangle, P.; Mintz, E.; Den Auwer, C.; Ferrand, M. *J. Biol. Inorg. Chem.* **2008**, *13*, 1239.
(27) Ralle, M.; Lutsenko, S.; Blackburn, N. J. *J. Biol. Chem.* **2003**, *278*, 23163.
(28) Voronova, A.; Meyer-Klaucke, W.; Meyer, T.; Rompel, A.; Krebs, B.; Kazantseva, J.; Sillard, R.; Palumaa, P. *Biochem. J.* **2007**, *408*, 139.
(29) Pushie, M. J.; Zhang, L. M.; Pickering, I. J.; George, G. N. *Biochim. Biophys. Acta, Bioenerg.* **2012**, *1817*, 938.
(30) Brown, K. R.; Keller, G. L.; Pickering, I. J.; Harris, H. H.; George, G. N.; Winge, D. R. *Biochemistry* **2002**, *41*, 6469.
(31) Graden, J. A.; Posewitz, M. C.; Simon, J. R.; George, G. N.; Pickering, I. J.; Winge, D. R. *Biochemistry* **1996**, *35*, 14583.
(32) Xiao, Z.; Loughlin, F.; George, G. N.; Howlett, G. J.; Wedd, A. G. *J. Am. Chem. Soc.* **2004**, *126*, 3081.
(33) George, G. N.; Winge, D.; Stout, C. D.; Cramer, S. P. *J. Inorg. Biochem.* **1986**, *27*, 213.
(34) George, G. N.; Byrd, J.; Winge, D. R. *J. Biol. Chem.* **1988**, *263*, 8199.
(35) Smith, T. A.; Lerch, K.; Hodgson, K. O. *Inorg. Chem.* **1986**, *25*, 4677.

(36) Pickering, I. J.; George, G. N.; Dameron, C. T.; Kurz, B.; Winge, D. R.; Dance, I. G. *J. Am. Chem. Soc.* **1993**, *115*, 9498.
(37) Riddles, P. W.; Blakeley, R. L.; Zerner, B. *Methods Enzymol.* **1983**, *91*, 49.
(38) Proux, O.; Nassif, V.; Prat, A.; Ulrich, O.; Lahera, E.; Biquard, X.; Menthonnex, J. J.; Hazemann, J. L. *J. Synchrotron Radiat.* **2006**, *13*, 59.
(39) Ravel, B.; Newville, M. *J. Synchrotron Radiat.* **2005**, *12*, 537.
(40) Baumgartner, M.; Schmalle, H.; Baerlocher, C. *J. Solid State Chem.* **1993**, *107*, 63.
(41) Chen, K.; Yuldasheva, S.; Penner-Hahn, J. E.; O'Halloran, T. V. *J. Am. Chem. Soc.* **2003**, *125*, 12088.
(42) Kau, L. S.; Spira-solomon, D. J.; Penner-Hahn, J. E.; Hodgson, K. O.; Solomon, E. I. *J. Am. Chem. Soc.* **1987**, *109*, 6433.
(43) Fujisawa, K.; Imai, S.; Kitajima, N.; Moro-oka, Y. *Inorg. Chem.* **1998**, *37*, 168.
(44) Lee, P. A.; Citrin, P. H.; Eisenberger, P.; Kincaid, B. M. *Rev. Mod. Phys.* **1981**, *53*, 769.
(45) Calculated with the same experimental procedure as the one used for $\mathbf{L}^1$ in ref 19.
(46) Gans, P.; Sabatini, A.; Vacca, A. *Talanta* **1996**, *43*, 1739.
(47) Newville, M. Data Processing with *IFFEFIT*, *ATHENA*, and *ARTEMIS*, Consortium for Advanced Radiation Sources, July 24, 2007, University of Chicago, Chicago, IL.
(48) Shannon, R. D. *Acta Crystallogr., Sect. A* **1976**, *A32*, 751.